

## Conducting block copolymers. Towards a polymer *pn*-junction

Frederik C. Krebs(✉), Mikkel Jørgensen

The Danish Polymer Center, RISØ National Laboratory, P.O. Box 49, 4000 Roskilde, Denmark

Received: 25 November 2002/Revised version: 10 April 2003/Accepted: 6 May 2003

### Summary

The synthesis of polyphenylacetylene (**1**), poly(pentafluorophenylacetylene) (**2**) and the block copolymer of **1** and **2** polyphenylacetylene-poly(pentafluorophenylacetylene) (**3**) using a Rhodium catalysed living polymerisation reaction is presented. Photoelectron spectroscopy of thin films of the individual polymers using 50eV photons from a synchrotron allowed for the determination of the position of the electronic energy levels, ionisation potentials and the vacuum level shift which indicated that the block copolymer organises at the gold substrate surface such that the fluorinated part of the copolymer extends towards the air interface. Pulse radiolysis time resolved microwave conductivity (PR-TRMC) allowed for the determination of the minimum carrier mobilities and the carrier lifetimes. The sum of carrier mobilities,  $\Sigma\mu_{\min}$ , were respectively  $5.2 \cdot 10^{-7}$ ,  $6.3 \cdot 10^{-7}$  and  $3.2 \cdot 10^{-7} \text{ m}^2 \text{ V}^{-1} \text{ s}^{-1}$  and the first half life,  $\tau_{1/2}$ , was 2.0, 1.5 and 1.0  $\mu\text{s}$  in **1**, **2** and **3**. The study shows that it is possible to make conducting block copolymers by the rhodium catalysed polymerisation of arylacetylenes with different electronic energies that organises at the surface giving rise to electronic properties that approach analogy to the traditional inorganic semiconductor pn-junctions.

### Introduction

The field of conducting polymers has received enormous attention recently due to major breakthroughs in their applicability to polymer based electronics [1], light emitting diodes [2] and all polymer photovoltaics [3] to mention a few centers of attention. The field of synthesis of conducting polymers has mostly been limited to homopolymers obtained by condensation polymerization [4] and only few examples of conducting polymer synthesis by living polymerisation has been presented [5,6]. Efficient synthetic procedures leading to conducting block copolymers is of large interest for several reasons aside from the synthetic challenge. The major reason being the ability to make block copolymers where the individual blocks have differing energy levels and different carrier transport properties thereby making it possible to create polymer based analogues of the well known inorganic *pn*- semiconductor junctions that are used in traditional inorganic semiconductor diodes and transistors etc.

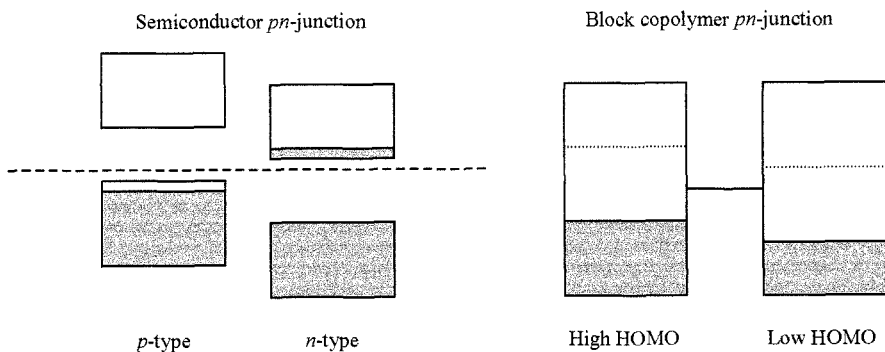
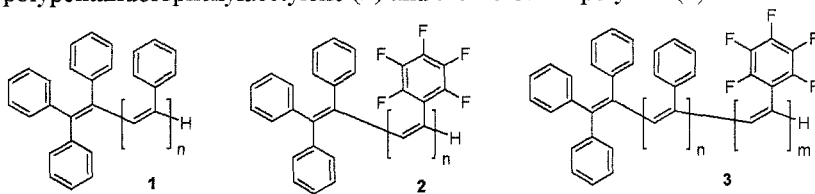


**Figure 1.** An illustration of the analogy between a traditional semiconductor *pn*-junction (left) and the block copolymer *pn*-junction (right) at thermal and electrical equilibrium. In the semiconductor version on the left the Fermi levels align at equilibrium. Any change from equilibrium by application of a bias or by illumination leads to the well known rectifying properties or photovoltaic response of the *pn*-junction. The analogous conducting polymer *pn*-junction (left) realised as a conducting block copolymer can have occupied and unoccupied energy levels with different positions on an absolute energy scale and is realised by two covalently bonded polymer blocks (indicated by the horizontal line between the two rectangles). The dotted line indicates the vacuum level of the polymer material. The position of the conduction band (LUMO) most often extend from somewhere below the vacuum level to above the vacuum level.

The position of the energy levels and the carrier transport in inorganic semiconductors relies on the nature of the bulk semiconductor material and the impurities introduced by doping. In the organic and polymer based systems the position of the energy levels is governed by the degree of orbital overlap or conjugation and the inductive properties of the substituents both of which also has some influence on the band gap. Fluorine substitution for instance has large electron withdrawing inductive properties and has been documented to lower the absolute position of the energy levels in conducting polymers [7]. Fluorine substitution has also in some cases been shown to change the nature of the carrier type in a conducting polymer from hole type (*p*-type) to electron type (*n*-type) [8]. While synthetic procedures leading to truly conducting block copolymer systems have not been reported Misumi et al. recently presented a living polymerisation reaction suitable for the polymerisation of phenylacetylene based on a Rhodium catalyst thus potentially making the synthesis of a conducting block copolymer possible [5].

In this paper we present the physical properties of polyphenylacetylene (**1**) pertaining to conducting polymer research, the synthesis and properties of poly(pentafluorophenylacetylene) (**2**) and their block copolymer (**3**).



Scheme 1. Homo-polymers **1** and **2** and block-copolymer **3**.

The interest in **1** and **2** being the demonstration of a lower position of the energy levels for **2** than for **1**. The block copolymer **3** should behave like a polymer *pn*-junction provided that the carrier mobility properties for the two polymers is such that

**1** favours hole transport (*p*-type) and that **2** favours electron transport (*n*-type). Even though strict *p*-type and *n*-type conduction is not adhered to for molecular systems when compared to their inorganic counterparts the system presented here serves as a demonstration of two potentially different conduction pathways for the holes and the electrons.

## Experimental

**Synthesis.** All commercially available reagents were purchased from Aldrich. Pentafluorophenylacetylene was synthesized as described in the literature [9]. Size exclusion chromatography (SEC) was performed in THF at 60 °C using a polystyrene calibration standard. <sup>19</sup>F NMR spectra were obtained for **2** and the block-copolymer **3** in 1,2-dichlorobenzene-*d*<sub>4</sub> at 430 K resulting in broad, but identifiable signals falling in three regions expected from the *o*-, *m*- and *p*-positions of the pentafluorophenyl groups. <sup>1</sup>H and <sup>13</sup>C spectra were also run, but contained no identifiable signals. At the elevated temperature necessary to dissolve these polymers all the signals in the <sup>1</sup>H spectra coalesced into a broad signal centered around 7.2 ppm. <sup>1</sup>H spectra of **1** were run in both CDCl<sub>3</sub> at 300K and in C<sub>6</sub>D<sub>4</sub>Cl<sub>2</sub> at 430 K. A well-resolved spectrum was obtained in CDCl<sub>3</sub> while a broad signal overlain with a few weak peaks was seen in the C<sub>6</sub>D<sub>4</sub>Cl<sub>2</sub> spectrum. The failure to obtain <sup>13</sup>C spectra can be explained from the large multiple couplings between <sup>19</sup>F and <sup>13</sup>C normally observed together with the line broadening intrinsic to many polymers.

**Polyphenylacetylene (1).** The polymer was prepared following the procedure described in ref. 5 and obtained as a bright yellow solid in 95 % yield.  $M_p = 15300$ ;  $M_n = 11300$ ;  $M_w/M_n = 1.23$ ; <sup>1</sup>H NMR (250.1 MHz, CDCl<sub>3</sub>, 300K)  $\delta$ : 5.86 (s, 1H), 6.6-6.7 (m, 2H), 6.9-7.0 (m, 3H); <sup>13</sup>C NMR (62.9 MHz, CDCl<sub>3</sub>, 300K)  $\delta$ : 126.7, 127.6, 127.8, 131.8, 139.4, 142.9 ppm.

**Poly(pentafluorophenylacetylene (2).** The polymer was prepared following the procedure described in ref. 5. using pentafluorophenylacetylene as the monomer. The polymer material was obtained as a dark yellow solid in 82% yield.  $M_p = 6200$ ;  $M_n = 3720$ ;  $M_w/M_n = 1.62$ ; <sup>19</sup>F NMR (235.3 MHz, C<sub>6</sub>D<sub>4</sub>Cl<sub>2</sub>, 430K)  $\delta$ : -163.4 (broad singlet), -153.6 (broad singlet), -141 to -137.3 (m) ppm.

**Polyphenylacetylene-poly(pentafluorophenylacetylene) block copolymer (3).** The polymer was prepared following the procedure described in ref. 5. Firstly, adding phenylacetylene and allowing for a reaction time of 1 hour. Pentafluorophenylacetylene was then added and the reaction left overnight at room temperature. The polymer was obtained as a dark brown solid in 87% yield.  $M_p = 7280$ ;  $M_n = 3000$ ;  $M_w/M_n = 2.61$ ; <sup>19</sup>F NMR (235.3 MHz, C<sub>6</sub>D<sub>4</sub>Cl<sub>2</sub>, 430K)  $\delta$ : -163.4 (broad singlet), -154.1 (broad singlet), -153.3 (broad singlet), -141 to -137.2 (m) ppm.

**Photoelectron spectroscopy.** The samples for ultraviolet photoelectron spectroscopy measurements (UPS) were prepared by spincoating a 1 mg mL<sup>-1</sup> solution of **1**, **2** and **3** in 1,2-dichlorobenzene onto a freshly prepared (by sputtering) polycrystalline gold substrate. The samples were then dried in a vacuum oven at 50 °C for 24h. The photoelectron spectra were recorded at the ASTRID storage ring at Aarhus University, Denmark. The beamline consists of an SX-700 monochromator and a hemispherical electron energy analyser. An ESCA (Electron Spectroscopy for Chemical Analysis) of the samples was recorded first to check the cleanliness of the area where the incident photons illuminated the sample and to confirm the presence of the elements (C for **1**, C and F for **2** and **3**) and the absence of the elements P, Rh and Cl. The photoelectrons

were measured at an angle normal to the sample surface. The ESCA scans were performed with 800eV photons and a resolution of 0.4 eV. The photoelectron spectra were recorded using 50eV incident photons and a resolution of 0.2 eV. The sample holder was kept at a potential of  $-9.5V$  relative to the surrounding instrument to eliminate the contribution from the instrument work function at the low energy cut-off. A clean gold substrate was first entered and sputtered for 1 hr with ionised argon using an emission current of 22 mA and a potential of 3 kV. The samples of **1**, **2** and **3** were introduced and the photoelectron spectra recorded. The onset and cut-off of the intensity normalised photoelectron spectra were used to compute the work function in the case of the pure gold substrate and the ionisation potential and valence band edge in the case of the gold substrates containing the samples. The data are presented in table 1. The gold work function,  $\Phi_{Au}$ , was determined to be 5.3 eV. The position of the valence band edge for **1**, **2** and **3**,  $E_F^{VB}$ , was lower than the Fermi level of gold. The Fermi level in compounds **1**, **2** and **3** are thus situated in the forbidden band gap of the materials and the distance from the Fermi level of the samples to the vacuum level is given by the difference between the ionisation potential, IP, and  $E_F^{VB}$  giving  $E_F^{VAC}$ . The vacuum level shift,  $\Delta$ , is thus obtained as:  $\Delta = E_F^{VAC} - \Phi_{Au}$ . The vacuum level shift reflects how the molecules orient at the surface giving a dipole layer. The procedure employed in the analysis of the data has been reported [7,10].

**Conductivity.** The technique employed for the determination of carrier mobilities was the well-known pulse radiolysis time resolved microwave conductivity technique (PR-TRMC) [11]. The technique relates a measured change in reflected microwave power from the sample to the conductivity change upon passage of high-energy electrons. From the transient changes in conductivity the lifetime of the carriers can be determined as well as the sum of the mobility of the carriers. The advantage of the technique is that the magnitude of the carrier mobility obtained is the minimum average carrier mobility and it is independent of sample preparation i.e. no contact resistance. This means that even higher mobilities are likely for suitably oriented samples. A disadvantage is that it is the sum of carrier mobilities that is obtained and the technique does thus not allow for distinguishing between hole and electron mobilities. The system used the 10MeV electron accelerator facility at Risø National Laboratory where short pulses of electrons 10-500ns could be passed through the sample placed in an R-band waveguide (26.5-40GHz). Three microwave sources were employed. A HP8690B Sweeper with a HP8697A 26.5-40GHz module in conjunction with a broadband power amplifier. Two Gunn diode sources in the frequency range 31-35 GHz were employed when possible due to the high power (27dbm) and low noise obtained from these sources. The appropriate microwave source could be switched into the system that consisted of a 26.5-40GHz HP R532A frequency meter and a 26-40GHz HP R382A attenuator. Hereafter the microwaves were lead into the first port of a three-port circulator and from the second port to the sample holder that was placed in the path of the electron beam. The sample was evacuated to a pressure of  $10^{-5} - 10^{-4}$  mBar using a turbo pump during measurements. The reflected microwave power was again entering the second port of the circulator and taken from the third port through an isolator and a circular waveguide cavity filter (TE<sub>111</sub> bandpass filter with a bandwidth of 500MHz). At this point the reflected power could be switched into a power meter (HP432A with a HP R486A Thermistor Mount) for the absolute measurement of microwave power or directly to a HP R422C schottky barrier diode with a time response better than 1 ns. At this point the time response of

the system is limited by the bandwidth of the cavity filter ( $\sim 2$  ns). The fast transients were recorded in a  $50\Omega$  system on a 4Gs/s TDS784C oscilloscope from Tektronix. The electron beam was after passage through the sample picked up by a Faraday cup and used as the trigger source for the data collection. The electron pulse was used to monitor changes in beam current and pulse shape and to get a measure of the absorbed radiation dose per measured beam current. The conductivity was obtained by using a calibration curve relating the reflected microwave power as a function of detector diode output voltage. In order to extract the carrier mobility the number of carriers must be known. This was obtained from dosimetry where radiochromic films were used to get the distribution around the sample holder, and inside the sample holder in four depths using polyethylene spacers (this procedure followed the ASTM E1275 standard "Practice for use of a radiochromic film dosimetry system"). A better absolute measure of the dose was obtained using alanine pellets where the dose over the whole volume of the pellet is accurately determined (this procedure followed the ASTM E1607 standard "Practice for use of the alanine-EPR dosimetry system"). The typical dose for a 100 ns pulse was 25 Gy and the variation in dose over the sample volume was 10%. An analysis of the conductivity transient gave the carrier half-life,  $\tau_{1/2}$ . The results of the carrier mobility measurements are shown in table 2.

## Results and discussion

While the physics of conducting polymers in many ways are similar to metals and inorganic semiconductors there are some distinct differences. Most notably the often very one-dimensional nature of carrier transport in conducting polymers, the lack of a single mechanism by which the dopant determines the majority carrier type, no true band carrier motion, the dependence of the vacuum level on the organisation of the molecules at the surface and the undefined position of the Fermi level. Traditionally the Fermi level implies the position of the topmost filled electronic energy level. For conducting polymers, however, it can be found anywhere in the (forbidden) bandgap. The fundamental understanding needed before it becomes possible for conducting polymer materials to replace traditional semiconductors, includes control of the above mentioned distinctions and further the control of the positions of the energy levels, the carrier mobility, the type of carrier, the organisation of the material and most importantly flexible synthetic procedures leading to conducting polymer materials with the desired structure, properties and physical tractability.

**Synthesis.** The Rhodium catalysed living polymerisation reaction which works very well for phenylacetylene was employed using pentafluorophenylacetylene as the monomer giving the polymer poly(pentafluorophenylacetylene) (**2**). While **1** is quite soluble in most organic solvents the polymer **2** was found to show very little solubility where only boiling 1,2-dichlorobenzene was found to be a moderate solvent. Dilute solutions could be obtained in boiling THF which enabled SEC measurements (at 60 °C). When performing the polymerisation starting with phenylacetylene and then adding pentafluorophenylacetylene after the phenylacetylene had been consumed gave the block copolymer **3** which showed similar problems with solubility. The yields were similar to those for **1** which confirmed that the reaction runs quite well. The molecular structure for the polymer treated here are shown in scheme 1. The molecular weight determinations were difficult for both **2** and **3** due to the low solubility in common solvents and further the only indication of the molecular weights was based on SEC data (MALDI-TOF proved unfruitful in our hands). Since

molecular weights obtained from the SEC calibration curve (based on a series of polystyrene standards) is thus a relative measure. The hydrodynamic volume of the perfluorinated polymer in THF solution may be quite different to that of polystyrene and the indicated molecular weights thus of a different numeric value.

**Photoelectron spectroscopy.** The position of the electronic energy levels can be controlled by chemical substitution via two different mechanisms where either a purely inductive effect is used or a resonance effect. The desire is to be able to shift the energy levels up and down the energy scale without altering any other physical properties which in reality is very difficult to achieve. The inductive effect most easily allows for this and an example is the substitution of hydrogen for fluorine [7]. The resonance effect is most often accompanied with structural or conformational changes such as replacement of alkyl to alkoxy or amino as documented by Bredas et al. that treated how the positions of both filled and empty energy levels changes with substitution pattern [12].

In order to obtain two conducting polymers with significantly different energy levels that still allows for the same synthetic procedures to be employed we choose to substitute hydrogen for fluorine in **1** and thus obtained **2**. The inductive electron withdrawing effect of fluorine was shown to lower the level of the topmost filled levels as shown in table 1 where it can be seen that the highest occupied level electronic energy level (HOMO) for **2** is lower than that of **1** by 0.6 eV and the ionisation potential is somewhat higher for **2** as expected. For the block copolymer **3** the position of the topmost filled electronic energy level is higher than that of **1** which is unexpected. When, however, considering that the ionisation potential for **3** is very close to the ionisation potential observed for **2** and the much smaller vacuum level shift,  $\Delta$ , this could imply an organisation of the polymer molecules of **3** at the surface with the polyphenylacetylene part close to the gold substrate and the polypentafluorophenylacetylene part extending towards the air interface. The vacuum level shift is very sensitive to how the material is organised at the surface and the changes in sign of  $\Delta$  as a function of the molecular dipole has been reported and the findings here are consistent with the proposition that the polypentafluorophenylacetylene part of **3** extends towards air thus forming a weak dipole layer that also results in a similar raising of the flat band potential [13]. Further support of the organisation proposed above is found when considering an ESCA scan of the same region on the surface probed by UV photoelectron spectroscopy. This showed a composition near identical to the case of pure **2**.

**Table 1.** Data from the photoelectron spectra for the Au substrate and the polymers **1**, **2** and **3**.

Compound	$E_F^{VB}$	$E_F^{VAC}$	Cut-off	$\Delta$	IP
1	1.10	3.20	-45.70	-2.10	4.30
2	1.70	3.30	-45.00	-2.00	5.00
3	0.90	4.00	-45.10	-1.30	4.90

**Carrier mobilities.** Several methods for the determination of carrier mobilities have been reported. Examples are time of flight (TOF) [14], holographic time of flight (HTOF) [15], field effect mobilities (FET) [16] and DC measurements of the conductivity [17]. Common to all the above mentioned methods are that the result is extremely sensitive to the technical aspects and the particular issue of contact resistance that can influence the result by many orders of magnitude compared to the

variation in magnitude of the parameter of interest. The pulse radiolysis time resolved microwave conductivity technique (PR-TRMC) [11] is an example of a contact less method for the determination of the sum of carrier mobilities,  $\Sigma\mu_{\min}$ , the major advantage being the conservative nature of the technique which means that the value for the mobility sum obtained is the minimum possible value, secondly an indication of the carrier half life is also obtained directly from the experiment. A distinct (an perhaps the only) disadvantage is that one generally cannot distinguish the contribution from each of the carrier types (holes and electrons) towards the sum of carrier mobilities. An example where the individual carrier mobilities have been obtained from a PR-TRMC experiment has however been reported [18]. We choose the PR-TRMC method due to the contact less nature and that the figure obtained can justifiably be compared to values obtained for other materials by this method.

**Table 2.** The minimum sum of carrier mobilities  $\Sigma\mu_{\min}$  (based on a carrier pair formation energy of 25 eV) and the first half life  $\tau_{1/2}$ .

	$\Delta\sigma/(\rho D)$ ( $S m^2 J^{-1}$ )	$\Sigma\mu_{\min}$ ( $m^2 V^{-1} s^{-1}$ )	$\tau_{1/2}$ ( $\mu s$ )
<b>1</b>	$2.1 \times 10^{-8}$	$5.2 \times 10^{-7}$	2.0
<b>2</b>	$2.5 \times 10^{-8}$	$6.3 \times 10^{-7}$	1.5
<b>3</b>	$1.3 \times 10^{-8}$	$3.2 \times 10^{-7}$	1.0

The values obtained by this method for **1**, **2** and **3** are shown in table 2 and are typical of conducting polymers. For comparison, carrier mobilities obtained by this method for other polyacetylenes are nearly two orders of magnitude higher [19], one magnitude higher for poly-3-hexylthiophene [20] and similar to polyalkoxyphenylenevinylene derivatives [21]. The carrier mobility sum found for the conducting block copolymer **3** is slightly lower than for the homopolymers **1** and **2** and this is perhaps due to a different organisation of the material. The crystallinity and organisation of a material has a very large influence on the observed carrier mobility [22]. We ascribe the observation of a lower carrier mobility sum for the polyarylacetylenes presented here when compared to polyacetylenes to be due to the organisation of the material where the bulky aryl groups prevent an the efficient overlap and conjugation. The carrier lifetimes are in the microsecond range and slightly lower for **3** which most likely are due to the trapping states that arises dipolar nature of the block copolymer molecules.

## Conclusions

In this work we have presented the synthesis and characterisation of a new conducting block copolymer based on polyphenylacetylene and poly(pentafluorophenyl)acetylene prepared by Rhodium catalysed living polymerisation. We have further established the differences in electronic energy levels for these polymers by photoelectron spectroscopy and determined the sum of carrier mobilities in these systems by PR-TRMC. The material organises at the surface with the fluorinated blocks extending towards the air interface.

*Acknowledgements.* This work was supported by the Danish Technical Science Foundation of Denmark (STVF). We would like to express sincere gratitude to Torben Johansen for technical

assistance at the Accelerator beamline, Arne Miller and Hanne Corfitzen for the Dosimetry measurements, Jan Alstrup for performing the DSC measurements, Sokol Ndoni and Walther B. Pedersen for SEC measurements, Zheshen Li, Søren V. Hoffmann and Philip Hofmann for technical support at the ASTRID storage ring and at the beamline.

## References

1. Katz HE, Lovinger AJ, Johnson J, Kloc C, Siegrist, T, LiW, Lin, Y-Y, Dodabalapur A (2000) *Nature* 404:478. Drury CJ, Mutsaers CMJ, Hart CM, Matters M, de Leeuw DM (1998) *Appl. Phys. Lett.* 73:108. Siringhaus H, Tessler N, Friend RH (1998) *Science* 393: 619
2. Ho PKH, Kim J-S, Burroughes H, Becker SFY, Brown TM, Caclalli F, Friend RH (2000) *Nature* 404:408. Yang Y (1997) *Mater. Res. Soc. Bull.* 22:16.
3. Schön JH, Kloc C, Bucher E, Batlogg B (2000) *Nature* 403:408
4. Lahti PM, Modarelli DA, Denton FR, Lenz RW, Karasz FE (1988) *J. Am. Chem. Soc.* 110:7258. Lenz RW, Han C-C, Stenger-Smith J, Karasz FE (1998) *J. Pol. Sci. Part A* 26:3241. Benjamin I, Hong H, Avny Y, Davidov D, Neumann R (1988) *J. Mater. Chem.* 8:919
5. Misumi Y, Masuda T (1998) *Macromolecules* 31:7572
6. Kishimoto Y, Eckler P, Miyatake T, Kainosho M, Ono A, Ikariya T, Noyori R (1999) *J. Am. Chem. Soc.* 121:12035. Misumi Y, Kanki K, Miyake M, Masuda T (2000) *Macromol. Chem. Phys.* 201:2239
7. Krebs FC, Jørgensen M (2002) *Macromolecules* 35:7200
8. Facchetti A, Deng Y, Wang A, Koide Y, Siringhaus H, Marks TJ, Friend RH (2000) *Angew. Chem. Int. Ed.* 39:4547. Katz HE, Lovinger AJ, Johnson J, Kloc C, Siegrist T, Li W, Lin Y-Y, Dodabalapur A (2000) *Nature* 404:478
9. Knunyants IL, Yakobsen GG (1985) *Synthesis of Fluoroorganic Compounds*. Springer-Verlag, Berlin Heidelberg New York Tokyo
10. Salaneck WR, Lögdlund M, Fahlman M, Greczynski G, Kugler Th (2001) *Materials Science and Engineering R*34:121
11. Infelta PP, de Haas MP, Warman JM (1977) *Radiat. Phys. Chem.* 10:353. de Haas MP (1977) Ph. D. Thesis. University of Leiden. Warman JM (1982) in *The Study of Fast Processes and Transient Species by Electron Pulse Radiolysis*. Baxendale JH, Busi F Eds. Riedel, Dordrecht, pp129-161. Warman JM, de Haas MP (1991) in *Pulse Radiolysis of Irradiated Systems*, Tabata Y, Ed, CRC Press: Boca Raton, FL pp 101-133. Schouten PG, Warman JM, de Haas MP (1993) *J. Phys. Chem.* 97:9863
12. Brédas JL, Heeger AJ (1994) *Chem. Phys. Lett.* 217:506
13. Ishii H, Sugiyama K, Ito E, Seki K (1999) *Adv. Mater.* 11:605
14. Spear WE (1969) *J. Non-Cryst. Solids* 197. Lee CH, Yu G, Heeger AJ (1993) *Phys. Rev. B* 47:15543. Lee CH, Yu G, Moses D, Heeger AJ (1994) *Phys. Rev. B* 49:2396
15. Wolff J, Schlöter S, Hofmann U, Haarer D, Zilker SJ (1999) *J. Opt. Soc. Am. B* 16:1080
16. Horowitz G (1998) *Adv. Mater.* 10:365. Würthner F (2001) *Angew. Chem. Int. Ed.* 40:1037. Kraft A (2001) *ChemPhysChem* 163
17. Katz HE, Siegrist T, Schön JH, Kloc C, Batlogg B, Lovinger AJ, Johnson J (2001) *ChemPhysChem* 167
18. Hoofman RJOM, de Haas MP, Siebbeles LDA, Warman JM (1998) *Nature* 392:54
19. Hoofman RJOM, van der Laan GP, Siebbeles LDA, de Haas MP, Bloor D, Sandman DJ (2001) *Macromolecules* 34:474
20. de Haas MP, van der Laan GP, Wegewijs B, de Leeuw DM, Bäuerle P, Rep DBA, Fichou D (1999) *Synthetic Metals* 101:524
21. Gelinck GH, Warman J J. *Phys. Chem.* 100:20035
22. Siringhaus H, Brown PJ, Friend RH, Nielsen MM, Bechgaard K, Langeveld-Voss BMW, Spiering AJH, Janssen RAJ, Meijer EW, Herwig P, de Leeuw DM (1999) *Nature* 401:685